Influence of coastal upwelling and river discharge on the phytoplankton community composition in the northwestern Gulf of Mexico.

Sílvia Anglès[1,2,*], Antoni Jordi[3], Darren W. Henrichs[1], Lisa Campbell[1,4]

[1] Department of Oceanography, Texas A&M University, 3146 TAMU, College Station, TX 77843, USA

[2] Departament d'Ecologia i Recursos Marins, Institut Mediterrani d'Estudis Avançats, IMEDEA (UIB-CSIC), Miquel Marquès 21, 07190 Esporles, Mallorca, Spain

[3] Jupiter, 251 W 30th St, New York, NY 10001, USA

[4] Department of Biology, Texas A&M University, College Station, TX 77843, USA

Authors' email addresses:

Sílvia Anglès: angles.silvia@gmail.com

Antoni Jordi: antoni.jordi@jupiterintel.com

Darren W. Henrichs: dhenrichs@tamu.edu

Lisa Campbell: lisacampbell@tamu.edu

***Corresponding author:**

Sílvia Anglès: angles.silvia@gmail.com

Keywords:

Coastal circulation; Community Composition; Imaging FlowCytobot; Mississippi-Atchafalaya Rivers; Nutrient input; Stratification

Abstract

The regional circulation in the northwestern Gulf of Mexico during late spring-summer is modulated by upwelling-favorable winds that can cause coastal upwelling in the western region and by freshwater inputs from the Mississippi-Atchafalaya Rivers. Spatial variability and temporal dynamics of phytoplankton community composition were examined during two upwelling-favorable periods using data obtained with an Imaging FlowCytobot (IFCB) from two cruises on the Texas-Louisiana shelf in June 2013 and 2014 and from the Texas Observatory for Algal Succession Time series (TOAST) at Port Aransas (Texas). Phytoplankton spatial distributions were determined by the influence of upwelling and river discharged waters. In the 2013 cruise, upwelling was detected in a large portion of the western region and the phytoplankton assemblages were dominated by diatoms, mostly chain-forming taxa. As revealed by the TOAST time series, the upwelling onset caused a dramatic increase in diatom carbon biomass. In the areas not affected by upwelling, variation in the river plume distribution that resulted from the circulation and the different discharge magnitudes for each year influenced the spatial distributions of the phytoplankton community composition. Dinoflagellates and other flagellated taxa were notably dominant during the 2013 cruise, whereas both diatoms and flagellated groups dominated the assemblages during the 2014 cruise. High stratification promoted by freshwater input, notably higher during 2013 than 2014, likely favored the dominance of flagellated groups in 2013. This study provides evidence of the influence of coastal upwelling in the phytoplankton community of the northwestern Gulf of Mexico and contributes to the knowledge of the drivers of community composition in this high-productivity area.

1. Introduction

Marine phytoplankton play a central role in the planktonic food web and biogeochemical cycling in the global ocean. Primary production by phytoplankton is consumed or decomposed to support other trophic levels, including the fish we harvest, or exported to deeper waters. In marine ecosystems, the phytoplankton community is composed of assemblages of multiple species that coexist and have different strategies (Margalef 1978). A suite of tolerances and adaptations allows phytoplankton species to respond rapidly to changes in the environment and overcome growth limitation factors. These diverse life traits lead to species selection depending on the environmental factors, resulting in different species assemblages under different environmental regimes (Margalef 1978; Smayda et al. 2004). The composition and abundance of phytoplankton species influence the food web structure, transfer pathways and fluxes of organic matter (Michaels and Silver 1988). Therefore, knowledge of phytoplankton community composition and the processes that drive its variability is essential for understanding ecosystem functioning.

The Gulf of Mexico is a high productivity coastal region that supports abundant and diverse marine life and resources (Lohrenz et al. 1990; Lohrenz et al. 1999; Chen et al. 2000). Coastal waters of the northern Gulf of Mexico are influenced by the discharge of the Mississippi River and its distributary, the Atchafalaya River. The elevated nutrient input from these rivers, in complex interaction with factors such as light and mixing, sustains high phytoplankton biomass and primary production (Lohrenz et al. 1990; Lohrenz et al. 1999; Lehrter et al. 2009). Furthermore, nutrient-enhanced phytoplankton biomass, together with other factors such as light and nutrient limitation, freshwater inputs and other oceanographic processes that affect water column stability, control hypoxia in shelf bottom waters of the Gulf of Mexico (Rabalais et al. 2002; Di Marco et al. 2005; Sylvan et al. 2006; Bianchi et al. 2010; Fennel at al. 2011).

63 The magnitude of river freshwater discharge and seasonal patterns in regional and mesoscale
64 circulation drive the extent of the influence of the Mississippi and Atchafalaya Rivers on phytoplankton
65 biomass in the Gulf of Mexico (Müller-Karger et al. 1991; Chen et al. 2000). The shelf circulation is
66 primarily modulated by alongshore winds that vary seasonally (Cochrane and Kelly 1986; Nowlin et al.
67 1998). From fall to spring (September to May), wind is directed downcoast (west-southward) and
68 generates currents that extend the river plumes along the coast toward the Louisiana-Texas shelf. This
69 coincides with the typical seasonal pattern in freshwater discharge from the Mississippi and
70 Atchafalaya Rivers, in which discharge progressively increases from fall to its maximum in spring. In
71 summer months (June to August), the prevailing winds shift to upwelling favorable (north-
72 northeastward) and drive upcoast circulation that transport river waters toward the east and offshore,
73 where plume waters can be entrained beyond the shelf break by eddies and other mesoscale circulation
74 features (Cochrane and Kelly 1986; Müller-Karger et al. 1991; Walker et al. 2005). During this season,
75 freshwater discharge gradually decreases towards a minimum discharge in fall.

76 Previous studies based on historical hydrographic data, satellite imagery and numerical modeling have
77 identified cool waters along the western shelf due to deep water upwelling as a result of prevailing
78 north-northeastward winds during summer (Walker 2001; Walker et al. 2003; Zavala-Hidalgo et al.
79 2003, 2006). Injection of nutrients from deep waters to the surface promoted by upwelling favorable
80 winds is believed to play a role in supporting phytoplankton biomass and primary production in this
81 region (Müller-Karger et al. 1991; Sahl et al. 1993; Chen et al. 2000). In addition, other mesoscale
82 circulation features such as eddies shed from the Loop Current have been shown to stimulate
83 phytoplankton biomass through the vertical entrainment of nutrients as a result of their interaction with
84 the continental margin (Biggs 1992; Biggs and Müller-Karger 1994).

85 Most studies of the phytoplankton community composition in the northwestern Gulf of Mexico have
86 focused on the Mississippi River plume, while only a few have investigated the river-influenced areas

on the shelf and offshore (Fahnenstiel et al. 1995; Bode and Dortch 1996; Rabalais et al. 1996; Lambert et al. 1999; Schaeffer et al. 2012; Chakraborty and Lohrenz 2015). Previous findings showed that assemblages were largely influenced by light, stratification and nutrients, which produced changes in community composition with consequent impacts on productivity and carbon flux (Dortch and Whitledge 1992; Fahnenstiel et al. 1995; Lambert et al. 1998; Dagg and Breed 2003). Upwelling has been recognized as an important process in the northwestern Gulf of Mexico (Müller-Karger et al. 1991; Sahl et al. 1993; Chen et al. 2000); however, its potential influence on the phytoplankton community composition has not been described. In addition, the complex interaction between upwelling and river discharge modulates the extent of the influence of these two major forcings in the inner shelf, but the associated impacts on the phytoplankton communities in the Gulf of Mexico are largely unknown. Since phytoplankton species respond rapidly and selectively to changes in environmental factors, characterization of the community composition can help identify the mechanisms that drive responses in phytoplankton communities.

The objectives of this study were to investigate the spatial variability and temporal dynamics of phytoplankton community composition during upwelling-favorable periods in the northwestern Gulf of Mexico. We were also interested to examine how the phytoplankton community composition along the shelf responded as the influence of upwelling and river discharge conditions varied. To address these objectives, we analyzed the phytoplankton community composition acquired with an Imaging FlowCytobot (IFCB) during two cruises covering the Texas-Louisiana shelf in the northwestern Gulf of Mexico. To provide a broader temporal context for the cruise's observations, we also used data on phytoplankton community composition from the IFCB operating continuously at the Texas Observatory for Algal Succession Time series (TOAST) and associated oceanographic variables. Previously, the high temporal resolution of the TOAST time series was shown to be useful for

identifying phytoplankton community responses to storm events at the relevant temporal scales (Anglès et al. 2015).

2. Materials and methods

2.1. Study area and data collection

To study the horizontal spatial distribution of phytoplankton communities and associated environmental variables, two cruises were conducted in the Texas-Louisiana shelf (northwestern Gulf of Mexico) on board the *R/V Manta* from 20–25 June 2013 and 18–23 June 2014. For each cruise, sampling started at the westernmost station and continued eastward towards the Mississippi River mouth, and then headed westward in a zig-zag pattern from near the coast to offshore and back. Samples were collected from the surface (0.5–1 m) at 42 stations (Fig. 1) for phytoplankton and nutrient analysis. Phytoplankton samples were analyzed using an IFCB set up on board (see below). For nutrient analysis, samples were filtered through Whatman 25 mm GF/F filters and frozen (-20ºC) and analyzed ashore for nitrate (NO_3^-), nitrite (NO_2^-), ammonium (NH_4^+), phosphate (PO_4^-) and silicate (SiO_3^-) by standard autoanalyzer methods (WHPO 1994). Vertical profiles of temperature (ºC) and salinity (PSU) were recorded at each station using SeaBird SBE25 CTD. The Brunt-Väisälä frequency (N; s^{-1}) was derived from temperature and salinity vertical profiles using the formula $N = \sqrt{(g/\rho)\,(\partial\rho/\partial z)}$, where g is gravity, ρ is density and z is depth. The maximum frequency throughout the vertical profile was used as a measure of the stratification strength for each station.

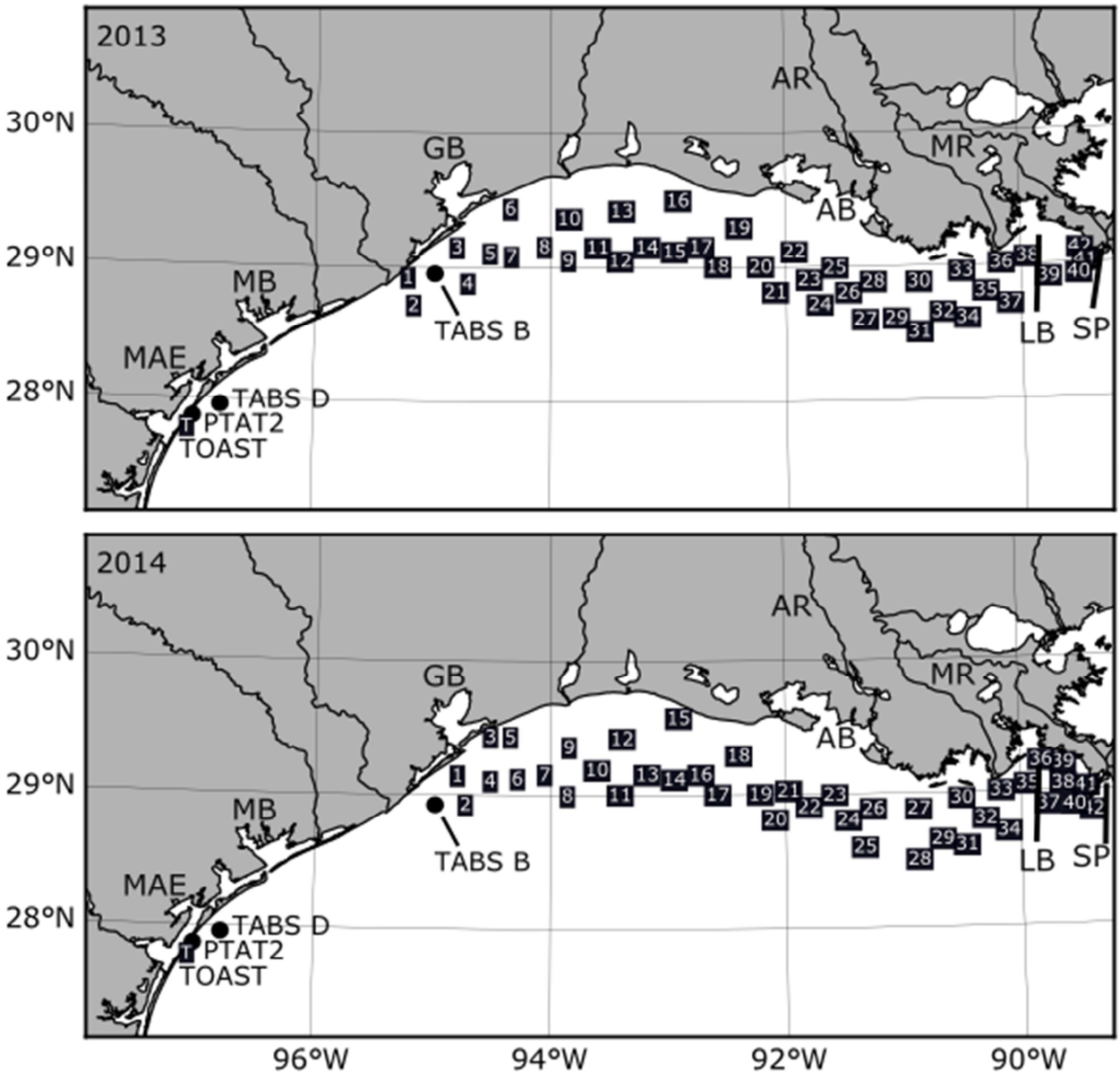

Figure 1. Maps of the northwestern Gulf of Mexico showing the sampling stations of the cruises in 2013 and 2014, the location of TOAST (T) in Port Aransas, the station PTAT2 and the buoys B and D (dots). Geographic locations: MAE = Mission-Aransas Estuary; MB = Matagorda Bay; GB = Galveston Bay; AB = Atchafalaya Bay; LB = Louisiana Bight; SP = Southwest Pass. Rivers: MR = Mississippi River; AR = Atchafalaya River.

As a reference for the temporal dynamics of the phytoplankton community during the periods of study,

we used the IFCB phytoplankton time series at TOAST in Port Aransas (Texas). The IFCB has been operating nearly continuously since September 2007 on the University of Texas Marine Science Institute (UTMSI) pier, located on the Port Aransas Ship Channel (27º 50.296'N, 97º 3.017'W; Fig. 1). This station is part of the Mission-Aransas National Estuarine Research Reserve (NERR) System Wide Monitoring Program. The Port Aransas Ship Channel is well-mixed with strong tidal currents. Tidal range is ~1.0 meter and the average water depth is 6.5 meters. Temperature and salinity at TOAST were obtained from the Mission-Aransas NERR Port Aransas Ship Channel station (http://cdmo.baruch.sc.edu/).

Wind speed and direction were obtained from station PTAT2, located near Port Aransas (Fig. 1) from the National Data Buoy Center (NDBC, http://ndbc.noaa.gov) and buoy B, located near Galveston Bay (Fig. 1) from the Texas Automated Buoy System (TABS, http://tabs.gerg.tamu.edu/). We use negative values of the alongshore wind component to indicate upwelling favorable winds and positive values to indicate downwelling favorable winds.

Water temperature was obtained from buoy D, located near Port Aransas (Fig. 1) and buoy B, located near Galveston Bay (Fig. 1) from TABS (http://tabs.gerg.tamu.edu/).

Satellite sea surface temperature (SST) was used to provide additional information on the spatial extent of upwelling in the study area following Chen et al. (2000), Walker (2001), Walker et al. (2003) and Zavala-Hidalgo et al. (2006). SST daily averages were obtained from the NOAA High Resolution SST dataset (OI SST, version 2; retrieved from https://climatedataguide.ucar.edu/climate-data/sst-data-noaa-high-resolution-025x025-blended-analysis-daily-sst-and-ice-oisstv2) provided by the NOAA/OAR/ESRL PSD (Boulder, Colorado, USA; http://www.esrl.noaa.gov/psd/; Banzon et al. 2017). Average SST for each cruise period at each grid point were calculated.

River discharge ($m^3 s^{-1}$) of the Mississippi and Atchafalaya Rivers were obtained from Tarbert Landing

158 and Simmesport stations, respectively, from the U.S. Army Corps of Engineers
159 (http://www.mvn.usace.army.mil/).

160 *2.2. Imaging FlowCytobot*

161 Phytoplankton community data were acquired with the IFCB, an instrument that combines flow
162 cytometry and video technologies to capture images of nano- and microplankton (~10 to ~150 µm) and
163 the associated fluorescence and light scattering signals (Olson and Sosik 2007). The IFCB analyzes 5
164 ml of seawater in ~20 min. For the cruises, at each station, 3 replicate 5-ml samples were run on an
165 IFCB set up on board. For the time series at TOAST, the standard configuration autonomous IFCB
166 analyzed a 5-ml sample of near-surface water every ~20 min. The IFCB was run continuously,
167 although there are a few gaps in the time series due to maintenance or electrical power failures.

168 The images generated by the IFCB were processed and classified automatically following the approach
169 described by Sosik and Olson (2007), with the modification of replacing the support vector machine for
170 machine learning with an assemblage of decision trees obtained by the random forest approach of
171 Breiman (2001). The automated classifier was created as described in Anglès et al. (2015). Briefly, a
172 training set of images for the automated classification was created with images (~300 for each plankton
173 category) selected from the IFCB image data sets. For this study, the automated classifier had 66
174 categories that were selected based on the community composition of plankton of the study area.
175 Categories were defined by morphology, so were either genus- or species-specific, or were composed
176 of groups of taxa with similar morphological characteristics. The classifier included 25 categories of
177 diatoms, 18 categories of dinoflagellates, 2 categories of cyanobacteria, 2 categories of haptophytes, 2
178 categories of raphidophytes, 1 category of dictyophytes, 1 category of chlorophytes, the category
179 Flagellates (chlorophytes, cryptophytes, prasinophytes, and euglenophytes), the category Other cells
180 (small cells that cannot be taxonomically identified from the images), 11 categories of protozoa

(including microzooplankton), and 2 categories to account for noncellular material (detritus and calibration beads). Of the 53 categories in the automated classifier that corresponded to phytoplankton, 29 were observed in the data during this study. Automated classification results from the cruise data were visually inspected and corrected manually.

To account for differences in cell size among phytoplankton species when assessing the relative contributions in mixed assemblages, carbon (C) biomass estimates were chosen as the metric for phytoplankton abundance (Smayda 1978; Hillebrand et al. 1999; Jakobsen et al. 2015). Cell volume calculations from the images, developed by Moberg and Sosik (2012), were used to obtain biovolume. Images of beads (9 μm, Duke Scientific Inc.) were used to obtain the pixel-μm factor to convert biovolumes into μm^3. C biomass estimations were then obtained from biovolume using the C conversion equations recommended by Menden-Deuer and Lessard (2000). We used $pgC\ cell^{-1} = 0.216 \times biovolume^{0.939}$ for all protists except for large diatoms (>3000 μm^3), for which we used $pgC\ cell^{-1} = 0.288 \times biovolume^{0.811}$ to account for the lower C content in these taxa due to the presence of intracellular vacuoles.

2.3. Statistical analyses

Spatial distribution patterns of similar phytoplankton community composition were assessed using Unweighted Pair Group Method with Arithmetic Mean (UPGMA) hierarchical agglomerative clustering based on a Bray-Curtis dissimilarity matrix, generated from the log-transformed (log+1) phytoplankton biovolume. Data from the TOAST time series was included using the average of biovolume during the cruise period for each year. One-way analysis of similarity (ANOSIM) was performed to confirm significant differences between the clusters. Principal Component Analysis (PCA) was applied to abiotic environmental variables to visualize patterns of variation and similarities across stations and to determine the relation between community composition and environmental

conditions for each of the cruises. Data were standardized prior to analysis. Statistical analyses were performed using the R statistical software (R Core Team, 2016) and the package vegan (Oksanen et al. 2017).

3. Results

3.1. Upwelling and freshwater discharge conditions

Wind data from the station PTAT2 (near Port Aransas) and TABS buoy B (near Galveston Bay) from June 2013 revealed upwelling-favorable winds during the 4 (near Port Aransas) and 6 (near Galveston Bay) days immediately preceding the June 2013 cruise (Fig. 2). In contrast, upwelling-favorable winds during June 2014 lasted a few days and occurred more than a week prior to the June 2014 cruise.

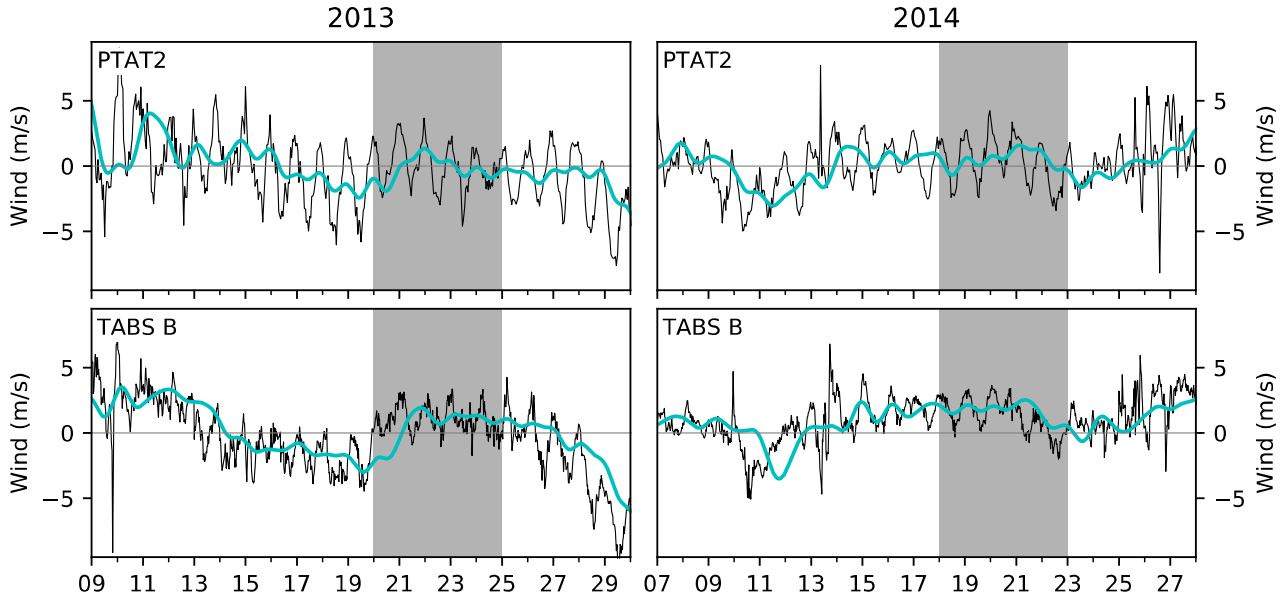

Figure 2. Alongshore wind component at PTAT2 and buoy B (see Fig. 1 for locations). Hourly (black line) and low-pass filtered (33-h; cyan line) data are represented. Negative values indicate upwelling favorable winds and positive values downwelling favorable winds. Cruise periods are marked by a gray bar.

Time series of temperature from TABS buoys D (near Port Aransas) and B (near Galveston Bay) from June 2013 showed decrease in temperature concurrent with the development of upwelling-favorable winds (Fig. 3). In 2013, temperatures reached the lowest values of ~26ºC and ~28ºC near Port Aransas and Galveston Bay respectively, and remained fluctuating around these values during the cruise dates. In 2014, the decrease in temperature was less pronounced, most of all near Galveston Bay, and temperatures were increasing during the dates when the cruise was conducted.

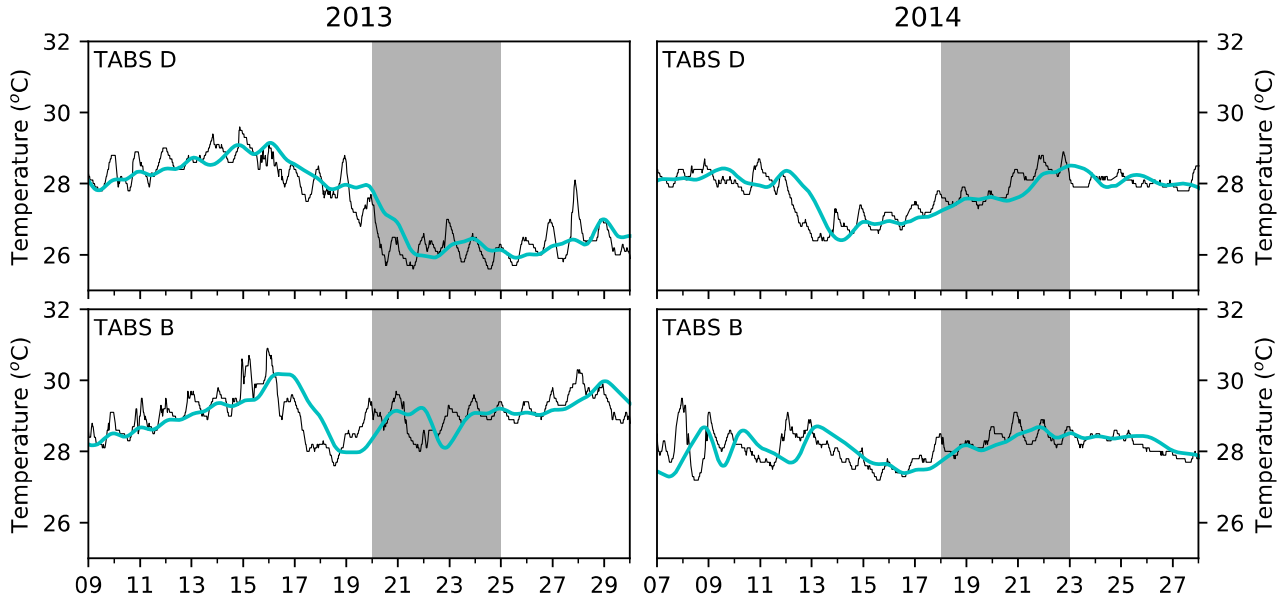

Figure 3. Water temperature at buoys D and B (see Fig. 1 for locations). Semi-hourly (black line) and low-pass filtered (33-h; cyan line) data are represented. Cruise periods are marked by a gray bar.

Average satellite SST during both cruises showed presence of cool water along the southwestern Texas-Louisiana shelf shore with variable spatial extent (Fig. 4). In this area, cool water along the shore that extends from Mexico to Texas is indicative of upwelling (Chen et al. 2000; Walker 2001; Walker et al. 2003; Zavala-Hidalgo et al. 2006). Cool water extended eastward up to Galveston Bay during 2013, whereas it did not reach further than Matagorda Bay (located south of Galveston Bay) during June 2014. These cool temperatures contrasted with the higher values over the mid and outer

shelf. In general, mid and outer shelf temperatures were higher in 2013 than 2014 (note the different scale in Fig. 4).

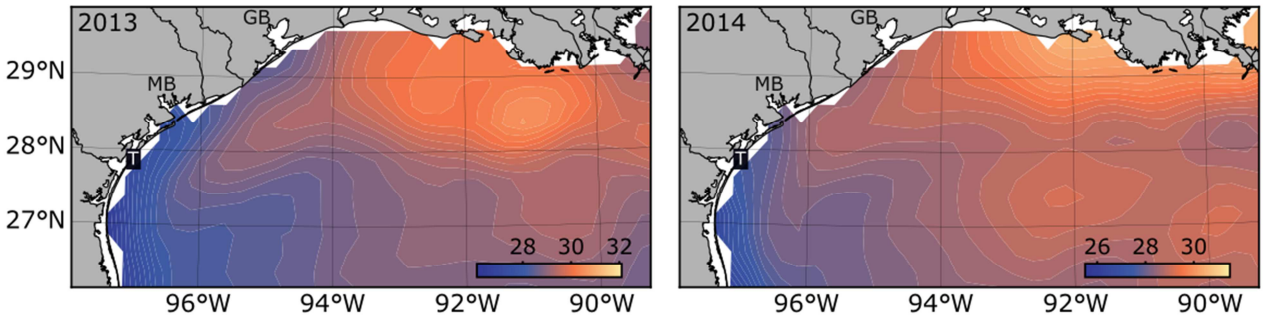

Figure 4. Satellite sea surface temperature (SST) average (^{o}C) for the cruise period in 2013 and 2014 (note that different scales were used for each period to account for temperature differences between years). Contours were generated using kriging interpolation method. Locations of TOAST (T) in Port Aransas, Matagorda Bay (MB) and Galveston Bay (GB) are indicated.

Considering the development of upwelling favorable-winds, the associated decreases in water temperature and the presence of cool waters along the shore visible from satellite SST, all these observations suggest that upwelling of variable strength and extent occurred during our study.

Freshwater discharge from the Mississippi and Atchafalaya Rivers was higher during May and June 2013 (26808 and 22968 m^3 s^{-1}, respectively, for the Mississippi River, and 11345 and 9812 m^3 s^{-1}, respectively, for the Atchafalaya River) compared to 2014 (17827 and 16479 m^3 s^{-1}, respectively, for the Mississippi River, and 7636 and 7091 m^3 s^{-1}, respectively, for the Atchafalaya River). Discharge during both May and June 2013 was higher than the 40-year (1975– 2014) average (21305 and 18291 m^3 s^{-1}, respectively, for the Mississippi River, and 9272 and 7940 m^3 s^{-1}, respectively, for the Atchafalaya River), while discharge during May and June 2014 was lower.

3.2. Spatial environmental variables during the cruises

The cruise periods spanned conditions of variable upwelling and magnitude of river freshwater discharges. The June 2013 cruise was conducted just after a long period of upwelling favorable winds and cool waters were observed up to Galveston Bay during the cruise dates. Therefore, upwelling was present in the western portion (the Galveston Bay region) of the area surveyed in the cruise. In June 2014, the period of upwelling favorable winds preceded the cruise, occurring much earlier and for a shorter duration, and cool waters did not extend to Galveston Bay during the cruise dates; consequently, upwelling was not present in the area surveyed in the cruise. In addition, freshwater discharges were substantially higher before and during the cruise in 2013 than in 2014.

Temperature and salinity recorded during the cruises reflected the influence of upwelling-favorable winds and the distribution of river plume waters under the different freshwater discharge conditions (Fig. 5). In 2013, a water mass of cool temperature (~28ºC) and high salinity (>30 PSU) was present in the Galveston Bay area. This cooler temperature contrasted with warmer temperature (>30ºC) over most of the shelf, except for the Mississippi River mouth (Southwest Pass), although values were not as low as in the Galveston Bay area. These observations agree well with the SST data that showed presence of cool water along the shore and further support the presence of upwelling in this area. There was a gradient of high to low salinity from west to east, with salinities <25 PSU in the middle and eastern shelf. The lowest salinity values were observed in the Mississippi River region (Louisiana Bight and Southwest Pass; ~7–10 PSU) and southeastward from Atchafalaya Bay (~17 PSU).

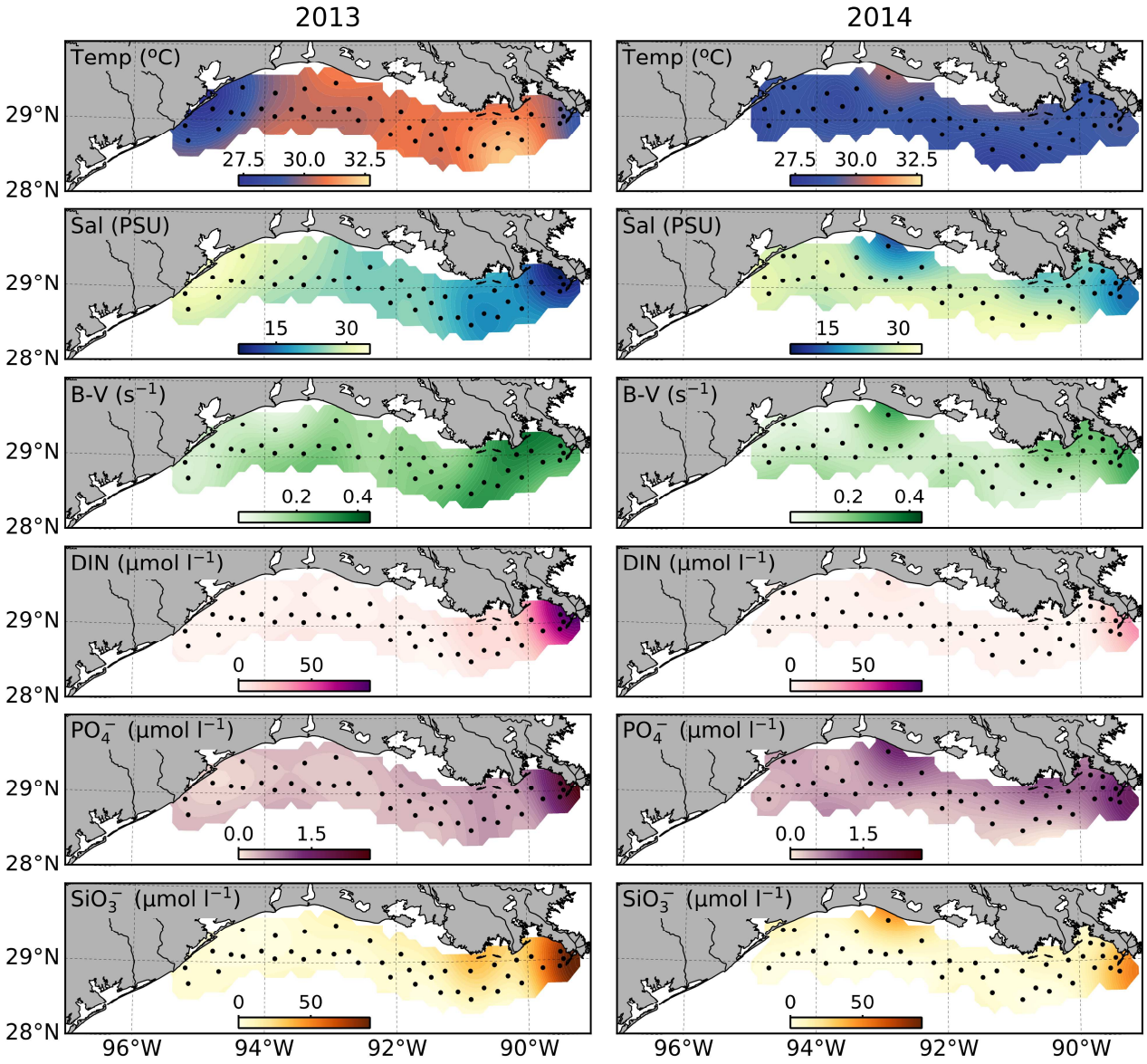

Figure 5. Maps of surface temperature (Temp), salinity (Sal), maximum Brunt-Väisälä frequencies (B-V), dissolved inorganic nitrogen (DIN), phosphate (PO_4^-) and silicate (SiO_3^-) contours using kriging interpolation for the cruise in 2013 and 2014. Station locations are indicated by dots.

In 2014, there was no indication of upwelling in the Galveston Bay area (Fig. 5), in agreement with the satellite SST that showed that cooler waters did not extend to Galveston Bay. Temperature was rather uniform in most of the shelf, with cooler temperatures (<30ºC) compared to 2013. Higher temperatures were observed near the coast, mainly west of Atchafalaya Bay. Due to the low river freshwater

discharge (lower than the long-term average) salinities were relatively high in the Mississippi River region (15–25 PSU) compared to 2013, with lower values found near the river mouth. The lowest salinity was observed in the near shore area west of Atchafalaya Bay (~10 PSU). In the rest of the shelf, salinity ranged between 25–34 PSU, with values ~30 PSU in most of the shelf.

Overall, stratification over the shelf was stronger in 2013 than in 2014 (Fig. 5). In 2013, maximum Brunt-Väisälä frequencies were >0.1 s^{-1} over the middle and eastern shelf, with the highest values in the Mississippi-Atchafalaya Rivers area. The exception was the western area affected by the upwelling, which showed frequencies <0.1 s^{-1}. In contrast, Brunt-Väisälä frequencies were <0.1 s^{-1} over most of the shelf during 2014. Frequencies >0.1 s^{-1} were observed nearshore in the middle and eastern shelf, with the highest frequencies found west of Atchafalaya Bay.

Spatial distributions of surface nutrient concentrations showed high concentrations of dissolved inorganic nitrogen (DIN=NO_3^-+NO_2^-+NH_4^+), PO_4^- and SiO_3^- in the vicinity of the Mississippi and Atchafalaya Rivers and lower to the west of the shelf during both cruises, except for another area of high nutrient concentrations near the shore west of Atchafalaya Bay in the 2014 cruise (Fig. 5). Overall, nutrient concentrations were higher during 2013 than 2014, particularly in the Mississippi River area, likely as a result of higher river discharge. During 2013, DIN, PO_4^- and SiO_3^- concentrations in the Mississippi River region were >40 μmol l^{-1}, >1 μmol l^{-1}, and >40 μmol l^{-1}, respectively, with the highest values in the Mississippi River mouth and decreasing westward. Nutrients were also high east of Atchafalaya Bay, where concentrations >20 μmol l^{-1}, >0.5 μmol l^{-1}, and >30 μmol l^{-1} were detected for DIN, PO_4^- and SiO_3^- respectively. Throughout the rest of the shelf, concentrations were <5 μmol l^{-1} for DIN, <0.5 μmol l^{-1} for PO_4^-, and <20 μmol l^{-1} for SiO_3^-. During 2014, DIN was 10-50 μmol l^{-1} in the Mississippi River region and west of Atchafalaya Bay, and <5 μmol l^{-1} over the rest of the shelf. Concentrations of PO_4^- and SiO_3^- were >1 μmol l^{-1} and >10 μmol l^{-1}, respectively, in the Mississippi River region and near the coast east and west of Atchafalaya Bay.

Peak concentrations were observed in the Mississippi River mouth and west of Atchafalaya Bay. Away from the coast, concentrations of PO_4^- and SiO_3^- were generally <0.8 μmol l^{-1} and <10 μmol l^{-1}, respectively, over the shelf.

3.3. Spatial distribution of phytoplankton community composition and relation with environmental variables

The phytoplankton community composition observed from the two June cruises was determined by the influence of upwelling and river discharged waters. Hierarchical clustering dendrograms based on Bray-Curtis dissimilarity revealed three clusters in 2013 and six clusters in 2014 that grouped distinct phytoplankton community assemblages (Fig. 6a). The ANOSIM analysis confirmed the significant differences between clusters (2013 cruise: $R = 0.83$, $p = 0.001$; 2014 cruise: $R = 0.78$, $p = 0.001$). For the 2013 cruise, cluster 1 grouped the stations in the low-salinity plume in the Mississippi-Atchafalaya Rivers region, whereas cluster 3 encompassed the stations located under the influence of upwelling in Galveston Bay and the nearest stations located eastward (Fig. 6b). Cluster 2 comprised the stations between the low-salinity plume and upwelling areas. Cluster 1 was characterized by high relative proportions of flagellated categories, mainly Other cells (which includes small cells that cannot be taxonomically identified from the images) and lower contributions of Flagellates, and Small dinoflagellates (Fig. 6c). Cluster 2 was largely represented by flagellated categories, mostly by the dinoflagellate *Prorocentrum texanum* followed by *Akashiwo* and Small dinoflagellates. Cluster 3 was characterized by a large proportion of diatom categories, primarily *Asterionellopsis* and *Chaetoceros* followed by *Rhizosolenia*, *Guinardia* and *DactFragCerataul* (category composed by *Dactyliosolen fragilissimus*, *Cerataulina pelagica* and *Leptocylindrus danicus*).

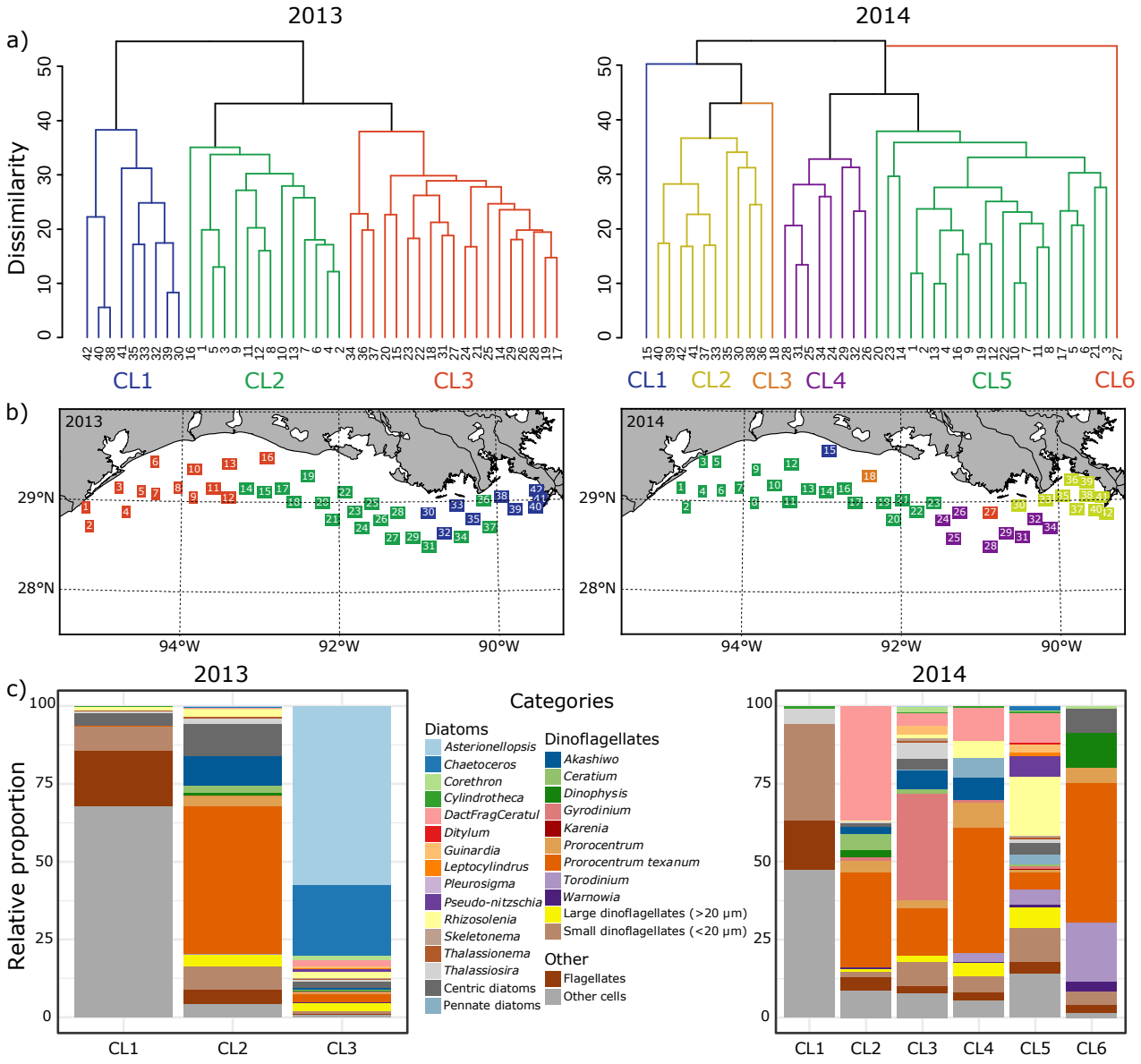

322

323 Figure 6. a) Hierarchical agglomerative clustering dendrograms representing Bray-Curtis dissimilarities
324 of the phytoplankton assemblages during the cruise in 2013 and 2014 (Cluster abbreviated as CL); b)
325 Maps of the distribution of the clusters according to the hierarchical agglomerative clustering analysis.
326 Stations belonging to each of the clusters are marked by color; c) Bar graphs showing the averaged C
327 biomass relative proportion of the phytoplankton categories in the assemblages of each cluster.

328 For the 2014 cruise, clusters 1 and 2 grouped mainly nearshore stations influenced by low-salinity
329 plume waters (Fig. 6b). Cluster 1 included the nearshore station located west of Atchafalaya Bay

(station 15), and cluster 2 grouped stations in the Mississippi River region. Cluster 3 included station 18, located near Atchafalaya Bay. The remaining stations were assigned to clusters 4 and 5, except for one station near the coast east of Atchafalaya Bay (station 27) that represented cluster 6. Cluster 1 was characterized by the flagellated groups Other cells, Small dinoflagellates and Flagellates (Fig. 6c). Cluster 2 was mostly represented by similar relative proportions of *DactFragCerataul* and *P. texanum*. In cluster 3, the dinoflagellate *Gyrodinium* showed the highest proportion in the assemblage. Cluster 4 was characterized by a high relative proportion of *P. texanum*, followed by *DactFragCerataul*, whereas in cluster 5 *Rhizosolenia*, Other cells, *DactFragCerataul* and Small dinoflagellates exhibited the largest proportions. Cluster 6 was mainly represented by flagellated categories, primarily *P. texanum* with important contributions of the dinoflagellates *Torodinium* and *Dinophysis*.

The grouping of the river influenced stations into one cluster (cluster 1) and the stations in the upwelling area into another cluster (cluster 3) in the 2013 cruise was supported by the PCA of the environmental variables (Fig. 7). PCA results revealed that the first component (component 1) explained 42% of the variance and highest loadings corresponded to salinity, DIN, SiO_3^- and PO_4^-. The highest positive scores of component 1 were found in the Mississippi-Atchafalaya Rivers area (Fig. 7), therefore representing the influence of river discharge and associated nutrients. The second component (component 2) accounted for 26% of the variance and temperature and Brunt-Väisälä frequency showed the highest loadings. The location of the highest positive scores corresponded to the area influenced by upwelling. For the 2014 cruise, the first component (45% of the variance), with highest loadings for salinity, SiO_3^- and PO_4^- , was related to river discharge since the corresponding highest positive scores corresponded to the Mississippi River area. The second component (20% of the variance) showed highest loadings for temperature, but the highest positive scores displayed a heterogeneous spatial pattern. We recall that no upwelling was observed in the area surveyed during the cruise in 2014.

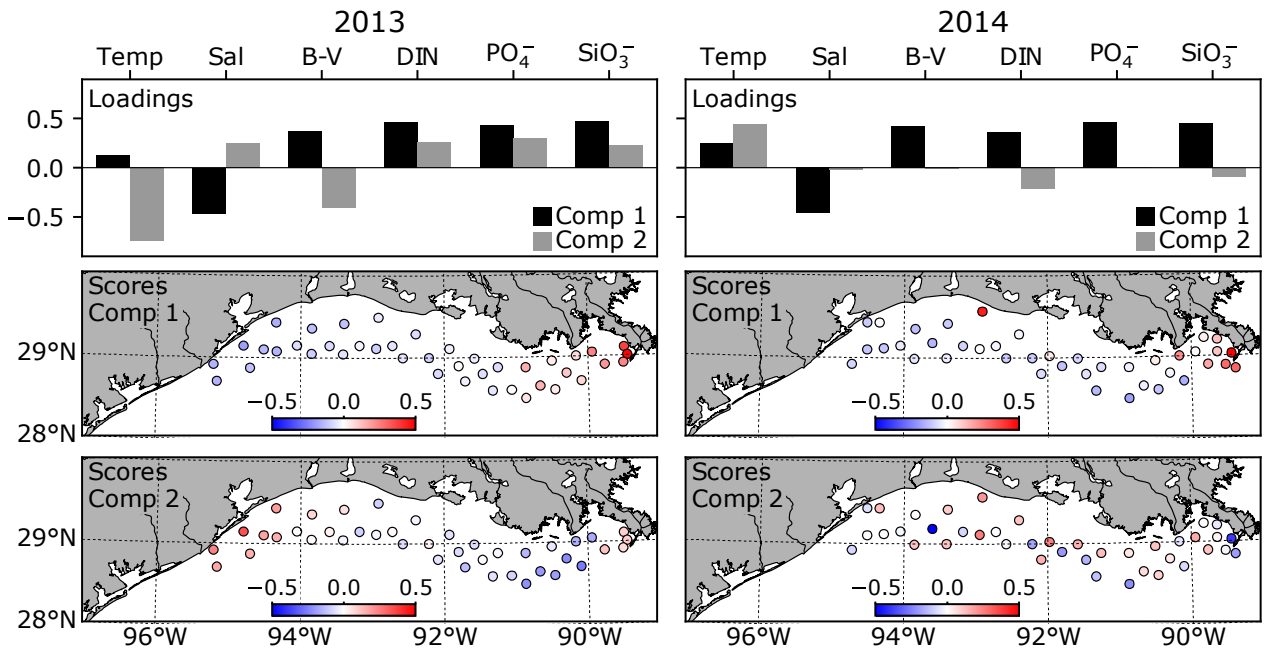

354

355 Figure 7. Principal Component Analysis (PCA) showing the patterns of variation in abiotic
356 environmental variables (temperature (Temp), salinity (Sal), maximum Brunt-Väisälä frequencies (B-
357 V), dissolved inorganic nitrogen (DIN), phosphate (PO_4^-) and silicate (SiO_3^-) across the stations for
358 the cruise in 2013 and 2014. Bars represent the loadings for PCA component 1 (Comp 1) and
359 component 2 (Comp 2). Maps illustrate the scores by station for each PCA component.

360 *3.4. Temporal dynamics of environmental variables and phytoplankton community composition at*
361 *TOAST in Port Aransas*

362 The IFCB phytoplankton time series at TOAST in Port Aransas and associated water temperature and
363 salinity were analyzed to characterize the temporal dynamics of these variables before and during the
364 cruises. Temperature and salinity showed the impact of the upwelling-favorable winds (Fig. 8). The
365 development of upwelling-favorable winds coincided with a decrease in temperature and an increase in
366 salinity in both years (see Fig. 2 for upwelling-favorable winds). In 2013, temperature decreased from
367 ~30 to ~26ºC, while salinity increased concurrently from ~27 to ~37 PSU. In 2014, the increase in

salinity was noticeable earlier than the decrease in temperature, and the fluctuations in both variables were smaller. While temperature decreased from ~29 to ~27ºC, salinity increased from ~33 to ~35 PSU. This change in temperature and salinity during the upwelling-favorable winds is consistent with the decrease in water temperature observed from the TABS buoy D (near Port Aransas) time series and satellite SST that showed presence of cool waters in Port Aransas for both years. These findings indicate that upwelling was present at Port Aransas (and therefore TOAST) before and during the period when the cruises were conducted.

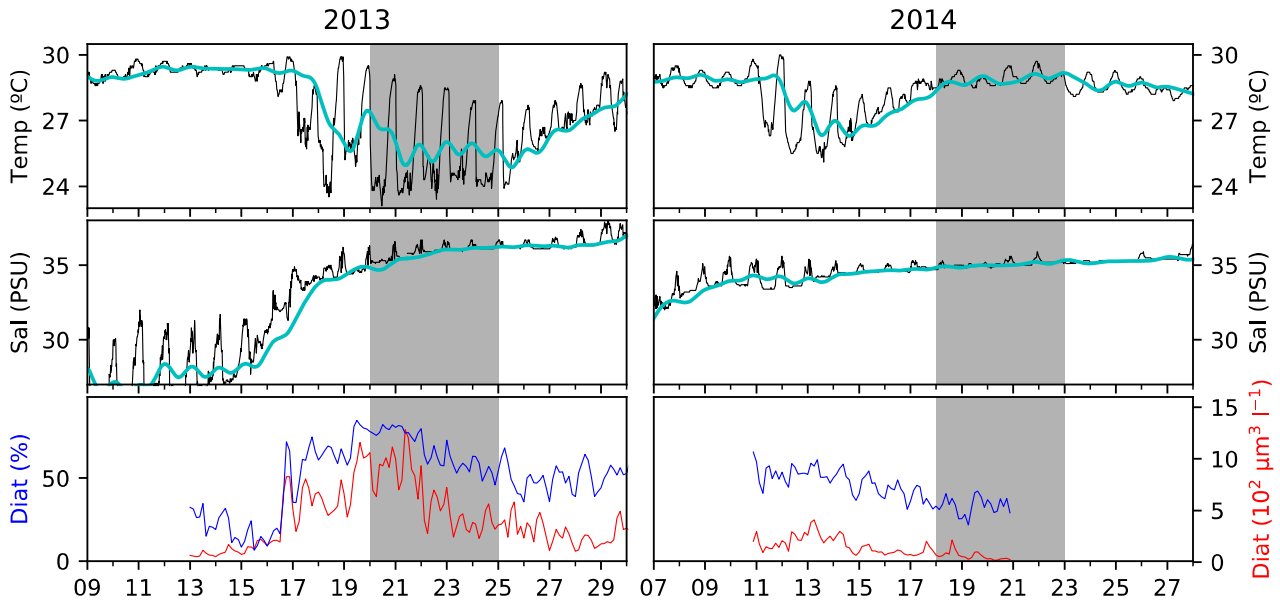

Figure 8. Temporal dynamics of temperature (Temp), salinity (Sal) and diatom (Diat) C biomass at TOAST. For temperature and salinity, raw (black line) and low-pass filtered (33-h; cyan line) data are shown. The total diatom C biomass is plotted (red line) along with diatoms as the percentage of the total phytoplankton C biomass (blue line). Cruise periods are marked by a gray bar.

Diatom categories (see Fig. 6c for the list of diatom categories) showed a dramatic increase in C biomass concurrent with the upwelling-favorable winds and change in temperature and salinity in 2013 (Fig 8). The dominant categories during the development of the upwelling-favorable winds were

383 *Asterionellopsis* and *Chaetoceros* (data not shown). In 2014, the upwelling-favorable winds coincided
384 with an IFCB data gap; thus, the response of the phytoplankton categories cannot be characterized.
385 Nevertheless, the diatom categories showed substantial C biomass during the development of the
386 upwelling-favorable winds. The contribution of diatoms to the total phytoplankton biovolume reached
387 up to 80% and 70% during the upwelling in 2013 and 2014, respectively.

388 **4. Discussion**

389 The contrasting oceanographic conditions in June 2013 and 2014 provided the opportunity to examine
390 the influence of regional circulation on phytoplankton community composition. The circulation during
391 these periods was modulated by the interaction between upwelling-favorable winds and freshwater
392 inputs from the Mississippi-Atchafalaya Rivers. Upwelling-favorable winds occurred for an extended
393 period immediately preceding the June 2013 cruise, while they occurred more than a week before the
394 June 2014 cruise and were shorter in duration. Consequently, upwelling occurred at TOAST in Port
395 Aransas and in the western part (Galveston Bay region) of the area surveyed during the 2013 cruise. In
396 contrast, while upwelling occurred at TOAST in Port Aransas, the area surveyed during the 2014 cruise
397 was not under the influence of upwelling. Freshwater inputs were also considerably different between
398 years: river discharge during May and June 2013 was higher than the 40-year (1975– 2014) average,
399 while it was lower during May and June 2014. Variations in upwelling-favorable winds and freshwater
400 inputs during both periods influenced the phytoplankton community composition in the study area.

401 Coastal upwelling on the western shelf of the Gulf of Mexico during summer has been described in
402 previous studies (Walker 2001; Walker et al. 2003; Zavala-Hidalgo et al. 2003, 2006). These studies
403 noted variability in the magnitude, duration, and spatial extent that depend on the intensity and
404 longevity of the northward wind during summer as well as on the intraseasonal variability of the wind
405 patterns. Upwelling-favorable winds (north-northeastward) cause upwelling of deep waters that result

406 in cool waters along the shore visible from satellite SST. Typically, cool waters extend from Mexico to
407 Matagorda Bay (see Fig. 1), but when upwelling is stronger than normal, cool upwelled waters are
408 observed farther northeast in Galveston Bay (Walker 2001). During our study, we observed north-
409 northeastward winds, which provided upwelling-favorable conditions. Further evidence of upwelling
410 included the decrease in temperature recorded at the buoys in Port Aransas and Galveston Bay area and
411 the decrease in temperature concurrent with an increase in salinity recorded at TOAST in Port Aransas
412 coinciding with the north-northeastward winds. In addition, satellite SST showed that cool waters along
413 the shore differed in spatial extent between the cruises and extended farther into the western portion of
414 the study area in 2013 (up to Galveston Bay) than in 2014 (up to Matagorda Bay). Cool waters
415 observed by satellite in the western portion (the Galveston Bay area) of the area surveyed in the 2013
416 cruise were in agreement with the cooler temperatures and higher salinities recorded at these stations in
417 the Galveston Bay area during that cruise.

418 The development of upwelling had a strong influence on the spatial distribution and structure of the
419 phytoplankton community. The phytoplankton assemblages at the stations under the influence of
420 upwelling during the 2013 cruise were dominated by diatoms, in particular, the chain-forming diatoms
421 *Asterionellopsis* and *Chaetoceros*. Observations at the high-resolution time series at TOAST in Port
422 Aransas, which provided a detailed characterization of the temporal changes in the phytoplankton
423 community composition during the upwelling events, revealed that the onset of upwelling caused a
424 shift to almost complete dominance of diatom categories in the total phytoplankton C biomass.
425 Dominance by *Asterionellopsis* and *Chaetoceros*, the same diatoms found at stations under the
426 influence of upwelling during the 2013 cruise, provided further evidence that the development of
427 upwelling influenced the phytoplankton composition and structure. Chain-forming diatoms tend to be
428 dominant in upwelling regions, and previous studies in upwelling areas report *Asterionellopsis* and
429 *Chaetoceros* as characteristic of coastal upwelled waters (e.g. Margalef 1978; Pitcher et al. 1991;

Tilstone et al. 2000; Lassiter et al. 2006), which supports our findings. Chain formation is a morphological adaptation that confers these diatom taxa an advantage in the turbulent conditions generated by upwelling (Smayda 1970). Their physiological features also provide a competitive advantage, since upwelling-adapted diatoms are able to respond earlier and faster to increases in nutrients, mainly of NO_3^-, compared to other phytoplankton taxa due to their high NO_3^- uptake rates (Malone 1980; Fawcett and Ward 2011).

At stations not affected by upwelling, freshwater inputs were the main drivers of the phytoplankton community. The extent of the river plumes over the shelf during each of the cruises influenced the spatial distributions and the composition of the phytoplankton assemblages. During periods of upwelling favorable winds, the upcoast circulation (eastward) extends the Atchafalaya River plume to the east-southward and presses the Mississippi River plume up against Southwest Pass and Louisiana Bight (Cochrane and Kelly 1986; Wiseman et al. 1997; Feng et al. 2014). If river discharge is high, the low-salinity plume waters and nutrients remain on the middle shelf (Feng et al. 2014). Our observations were in agreement; the low-salinity nutrient-rich plume waters were observed over the middle shelf during the June 2013 cruise, when river discharges were higher than normal. In contrast, the upcoast circulation and low river discharge conditions cause retention of low-salinity plume waters close to the coast near the freshwater sources (Nowlin et al. 2005; Walker et al. 2005; Schiller et al. 2011; Feng et al. 2014), which is consistent with our observations during the June 2014 cruise when river discharge was below the 40-year average. Under these conditions, our study revealed that flagellated groups dominated the overall community composition during the 2013 cruise, whereas diatoms were more prevalent in the 2014 cruise.

The dominance of flagellated groups in the 2013 cruise was somewhat surprising, however, as previous studies in the Mississippi River plume region and the shelf report that diatoms typically dominate the assemblages (Fahnenstiel et al. 1995; Bode and Dortch 1996; Rabalais et al. 1996; Lambert et al. 1999;

454 Dagg and Breed 2003; Chakraborty and Lohrenz 2015). A possible explanation for dominance by the
455 flagellated groups during the 2013 cruise was the strong water column stratification, which is known to
456 favor flagellated members of the phytoplankton community, as motile phytoplankton have the
457 advantage of remaining in the euphotic nutrient-rich zone. Freshwater input enhances density
458 stratification (Wiseman et al. 1997; Feng et al. 2014). Therefore, the high river discharge in 2013
459 promoted strong stratification over the middle and eastern shelf. These stratified conditions likely
460 favored the dominance of dinoflagellates in the middle shelf, where *P. texanum* was the primary
461 contributor to the assemblage followed by *Akashiwo* and Small dinoflagellates. In the eastern shelf,
462 where stratification reached the highest values, the community was dominated by Other cells,
463 Flagellates (cryptophytes, prasinophytes and euglenophytes), and Small dinoflagellates. Similar
464 assemblages dominated by cryptophytes, dinoflagellates, and chlorophytes were reported during peak
465 river discharge due to high stratification in the nearshore zone of the Mississippi-Atchafalaya Rivers
466 area (Schaeffer et al. 2012). In addition, increases in abundance of dinoflagellates, cryptophytes,
467 prasinophytes and euglenophytes were observed associated with high freshwater discharge and low
468 salinities previously at Port Aransas (Anglès et al. 2015).

469 During the 2014 cruise, our observations of the diatom group *DactFragCerataul* (composed by
470 *Dactyliosolen fragilissimus*, *Cerataulina pelagica* and *Leptocylindrus danicus*) in the assemblages of
471 the Mississippi River region support the findings of previous studies. Typically, high diatom biomass is
472 found at intermediate salinities (15-30 PSU) along the river plume (Dagg and Breed 2003), which
473 coincided with the salinities in this region (15-25 PSU). Notably, the dinoflagellate *P. texanum*
474 comprised a substantial fraction of the total phytoplankton in the Mississippi River region. This species
475 was dominant in the areas immediately adjacent, although its contribution to the assemblages did not
476 extend as far westward as in the cruise of 2013, which suggests that the spatial distribution of *P.*
477 *texanum* is largely influenced by the distribution of the river plume. *P. texanum* was described recently

by Henrichs et al. (2013), who reported high abundances of this species from Port Aransas during winter-spring. Our observations suggest that *P. texanum* is a common and widely distributed species in the northwestern Gulf of Mexico and the contribution of this species to the phytoplankton community in the Gulf of Mexico might be more important than previously thought. Elsewhere on the shelf, the assemblages were characterized primarily by the diatom *Rhizosolenia*. The presence of *Rhizosolenia* could be an indication of onshore flow of open Gulf of Mexico waters, since *Rhizosolenia* has been reported to be abundant in offshore waters of the northern Gulf of Mexico (Chakraborty and Lohrenz 2015).

Our detailed analysis of the spatial distribution of community composition revealed heterogeneous distributions of the phytoplankton assemblages at nearshore stations (i. e. stations 15, 18 and 27, see Fig 6 for 2014). These observed 'hot-spots' with distinctive taxonomic compositions are likely indicators of different environments with specific hydrographic conditions that influence the phytoplankton community.

6. Conclusions

Our study shows that the phytoplankton community composition in the northwestern Gulf of Mexico was shaped by two prominent processes of this environment, the freshwater input from the Mississippi-Atchafalaya Rivers and coastal upwelling. Distinct differences in these forcing factors were observed between years. Freshwater discharges were notably higher before and during the cruise in 2013 than in 2014, and the impact of upwelling extended farther into the western portion of the study area in 2013 than in 2014. The phytoplankton assemblages in the areas affected by upwelling were always dominated by chain-forming diatoms. In contrast, the community showed different responses in the areas influenced by freshwater input. During 2014, diatoms were more abundant in the phytoplankton assemblages of the river plume as reported by previous studies. However, dinoflagellates and other

501 flagellated taxa were more prevalent in these areas during the 2013 cruise. We suggest this shift was
502 likely due to increased stratification of the water column.

503 New insights provided by our study reveal a more complex picture of the phytoplankton community
504 composition of the Gulf of Mexico. The importance of dinoflagellates as a major component of the
505 phytoplankton community on the shelf in the northwestern Gulf of Mexico was unexpected. The most
506 common dinoflagellate species was the recently described *P. texanum*, which dominated a large part of
507 the shelf during both the 2013 and 2014 cruises. Our observations suggest that the contribution of
508 dinoflagellates to the total phytoplankton C biomass in the Gulf of Mexico might be more important
509 than previously thought. Since dinoflagellates present different C:N:P:Si cellular ratios than diatoms, a
510 more dinoflagellate-dominated system can influence the food web, the export fluxes and consequently
511 the benthic biogeochemistry (Spilling et al. 2018). However, the impact of dinoflagellate dominance in
512 the ecosystem functioning of the Gulf of Mexico region remains to be elucidated.

513 While the impact of the Mississippi-Atchafalaya Rivers on the phytoplankton community has been the
514 focus of attention in previous studies in this area of the Gulf of Mexico, data presented here identify
515 coastal upwelling as a driver of the phytoplankton community structure for the first time. The high
516 temporal resolution of the IFCB time series at TOAST enabled the identification of upwelling-induced
517 changes in the phytoplankton community composition. Although the magnitude, duration, and spatial
518 extent of the coastal upwelling in the northwestern Gulf of Mexico is variable, the influence of
519 upwelling on the phytoplankton community is likely a common phenomenon. Our study provides
520 further evidence of the influence that regional and mesoscale circulation features exert on planktonic
521 community composition (e. g. Williams et al. 2015). Future research should consider upwelling events
522 as an important driver of the phytoplankton community composition and determine the potential impact
523 of upwelling-induced responses in primary production and food web dynamics in the northwestern
524 Gulf of Mexico.

Acknowledgements

This research was supported by grants from a Marie Curie international outgoing fellowship (GA-302562) from the European Community to S.A., and NOAA/ECOHAB (NA09NOS4780196) and NOAA/PCMHAB (NA15NOS4780173) to L.C. We thank L. Harred for collecting the IFCB data during the cruises. We extend our gratitude to the crew of the *R/V Manta* for their assistance on the cruises, and to S. DiMarco for providing the environmental data from his NOAA/MCH cruises (NA09NOS4780208). We thank E. Buskey and the Mission-Aransas NERR program, the NOAA/OAR/ESRL PSD, the National Data Buoy Center and the Texas Automated Buoy System, and the U.S. Army Corps of Engineers for providing data of Port Aransas Ship Channel station, satellite SST, wind and water temperature, and freshwater discharge, respectively, and R. Mooney for technical assistance with the IFCB at TOAST.

References

Anglès, S., A. Jordi, and L. Campbell. 2015. Responses of the coastal phytoplankton community to tropical cyclones revealed by high-frequency imaging flow cytometry. Limnol. Oceanogr. 60: 1562–1576. doi:10.1002/lno.10117

Banzon, V., R. Reynolds, and National Center for Atmospheric Research Staff [eds.]. 2017. The Climate Data Guide: SST data: NOAA High-resolution (0.25x0.25) Blended Analysis of Daily SST and Ice, OISSTv2.

Bianchi, T. S., S. F. DiMarco, J. H. Cowan, R. D. Hetland, P. Chapman, J. W. Day, and M. A. Allison. 2010. The science of hypoxia in the Northern Gulf of Mexico: A review. Sci. Total Environ. 408: 1471–1484. doi: 10.1016/j.scitotenv.2009.11.047

Biggs, D. C. 1992. Nutrients, plankton, and productivity in a warm-core ring in the western Gulf of Mexico. J. Geophys. Res. 97: 2143. doi:10.1029/90JC02020

Biggs, D. C., and F. E. Müller-Karger. 1994. Ship and satellite observations of chlorophyll stocks in interacting cyclone-anticyclone eddy pairs in the western Gulf of Mexico. J. Geophys. Res. 99: 7371. doi:10.1029/93JC02153

Bode, A., and Q. Dortch. 1996. Uptake and regeneration of inorganic nitrogen in coastal waters influenced by the Mississippi River: spatial and seasonal variations. J. Plankton Res. 18: 2251 – 2268. doi: 10.1093/plankt/18.12.2251

Breiman, L. 2001. Random forests. Mach. Learn. 45: 5–32. doi:10.1023/A:1010933404324

Chakraborty, S., and S. E. Lohrenz. 2015. Phytoplankton community structure in the river-influenced continental margin of the northern Gulf of Mexico. Mar. Ecol. Prog. Ser. 521: 31–47.

557 doi:10.3354/meps11107

558 Chen, X., S. E. Lohrenz, and D. A. Wiesenburg. 2000. Distribution and controlling mechanisms of
559 primary production on the Louisiana-Texas continental shelf. J. Mar. Syst. 25: 179–207.
560 doi:10.1016/S0924-7963(00)00014-2

561 Cochrane, J. D., and F. J. Kelly. 1986. Low-frequency circulation on the Texas-Louisiana continental
562 shelf. J. Geophys. Res. 91: 10645. doi:10.1029/JC091iC09p10645

563 Dagg, M. J., and G. A. Breed. 2003. Biological effects of Mississippi River nitrogen on the northern
564 gulf of Mexico - A review and synthesis. J. Mar. Syst. 43: 133–152. doi:10.1016/j.jmarsys.2003.09.002

565 DiMarco S. F., W. D. Nowlin, and R. O. Reid. 2005. A statistical description of the velocity fields from
566 upper ocean drifters in the Gulf of Mexico, p. 101–110. In W. Sturges and A. Lugo-Fernandez [eds.],
567 Circulation in the Gulf of Mexico: Observations and models. AGU Geophysical Monograph Series,
568 161. doi: 10.1029/161GM08

569 Dortch, Q., and T. E. Whitledge. 1992. Does nitrogen or silicon limit phytoplankton production in the
570 Mississippi River plume and nearby regions? Cont. Shelf Res. 12: 1293–1309. doi:10.1016/0278-
571 4343(92)90065-R

572 Fahnenstiel, G. L., M. J. McCormick, G. A. Lang, D. G. Redalje, S. E. Lohrenz, M. Markowitz, B.
573 Wagoner, and H. J. Carrick. 1995. Taxon-specific growth and loss rates for dominant phytoplankton
574 populations from the northern Gulf of Mexico. Mar. Ecol. Prog. Ser. 117: 229–240.
575 doi:10.3354/meps117229

576 Fawcett, S. E., and B. B. Ward. 2011. Phytoplankton succession and nitrogen utilization during the
577 development of an upwelling bloom. Mar. Ecol. Prog. Ser. 428: 13–31. doi:10.3354/meps09070

578 Feng, Y., K. Fennel, G. A. Jackson, S. F. DiMarco, and R. D. Hetland. 2014. A model study of the
579 response of hypoxia to upwelling-favorable wind on the northern Gulf of Mexico shelf. J. Mar. Syst.
580 131: 63–73. doi:10.1016/j.jmarsys.2013.11.009

581 Fennel, K., R. Hetland, Y. Feng, and S. DiMarco. 2011. A coupled physical-biological model of the
582 Northern Gulf of Mexico shelf: Model description, validation and analysis of phytoplankton variability.
583 Biogeosciences 8: 1881–1899. doi: 10.5194/bg-8-1881-2011

584 Henrichs, D. W., P. S. Scott, K. A. Steidinger, R. M. Errera, A. Abraham, and L. Campbell. 2013.
585 Morphology and phylogeny of *Prorocentrum texanum* sp. nov. (Dinophyceae): A new toxic
586 dinoflagellate from the Gulf of Mexico coastal waters exhibiting two distinct morphologies. J. Phycol.
587 49: 143–155. doi:10.1111/jpy.12030

588 Hillebrand, H., C. -D. Dürselen, D. Kirschtel, U. Pollingher, and T. Zohary. 1999. Biovolume
589 calculation for pelagic and benthic microalgae. J. Phycol. 35: 403–424. doi: 10.1046/j.1529-
590 8817.1999.3520403.x

591 Jakobsen, H.H., J. Carstensen, P.J. Harrison, and A. Zingone. 2015. Estimating time series
592 phytoplankton carbon biomass: Inter-lab comparison of species identifications and comparison of
593 volume-to-carbon scaling ratios. Estuar. Coast Shelf Sci. 162: 143–150. doi:10.1016/j.ecss.2015.05.006

594 Lambert, C. D., T. S. Bianchi, and P. H. Santschi. 1998. Cross-shelf changes in phytoplankton
595 community composition in the Gulf of Mexico (Texas shelf/slope): The use of plant pigments as
596 biomarkers. Cont. Shelf Res. 19: 1–21. doi:10.1016/S0278-4343(98)00075-2

597 Lassiter, A. M., F. P. Wilkerson, R. C. Dugdale, and V. E. Hogue. 2006. Phytoplankton assemblages in
598 the CoOP-WEST coastal upwelling area. Deep. Res. Part II Top. Stud. Oceanogr. 53: 3063–3077.
599 doi:10.1016/j.dsr2.2006.07.013

Lehrter, J. C., M. C. Murrell, and J. C. Kurtz. 2009. Interactions between freshwater input, light, and phytoplankton dynamics on the Louisiana continental shelf. Cont. Shelf Res. 29: 1861–1872. doi.org/10.1016/j.csr.2009.07.001

Lohrenz, S. E., M. J. Dagg, and T. E. Whitledge. 1990. Enhanced primary production at the plume/oceanic interface of the Mississippi River. Cont. Shelf Res. 10: 639–664. doi:10.1016/0278-4343(90)90043-L

Lohrenz, S. E., G. L. Fahnenstiel, D. G. Redalje, G. A. Lang, M. J. Dagg, T. E. Whitledge, and Q. Dortch. 1999. Nutrients, irradiance, and mixing as factors regulating primary production in coastal waters impacted by the Mississippi River plume. Cont. Shelf Res. 19: 1113–1141. doi:10.1016/S0278-4343(99)00012-6

Malone, T. C. 1980. Size-fractionated primary productivity of marine phytoplankton, p. 301–319. In P.G. Falkowski [ed.], Primary productivity in the sea. Plennum Press. doi: 10.1007/978-1-4684-3890-1_17

Margalef, R. 1978. Life-forms of phytoplankton as survival alternatives in an unstable environment. Oceanol. Acta 1: 493–509. doi:10.1007/BF00202661

Menden-Deuer, S., and E. J. Lessard. 2000. Carbon to volume relationships for dinoflagellates, diatoms, and other protist plankton. Limnol. Oceanogr. 45: 569–579. doi:10.4319/ lo.2000.45.3.0569

Michaels, A. F., and M. W. Silver. 1988. Primary production, sinking fluxes and the microbial food web. Deep Sea Res. Part A, Oceanogr. Res. Pap. 35: 473–490. doi:10.1016/0198-0149(88)90126-4

Moberg, E. A., and H. M. Sosik. 2012. Distance maps to estimate cell volume from two-dimensional plankton images. Limnol. Oceanogr. Methods 10: 278–288. doi:10.4319/lom.2012.10.278

621 Müller-Karger, F. E., J. J. Walsh, R. H. Evans, and M. B. Meyers. 1991. On the seasonal phytoplankton
622 concentration and sea surface temperature cycles of the Gulf of Mexico as determined by satellites. J.
623 Geophys. Res. 96: 12645. doi:10.1029/91JC00787

624 Nowlin, W. D., A. E. Jochens, R. O. Reid, and S. F. DiMarco. 1998. Texas- Louisiana Shelf circulation
625 and transport processes study: Synthesis report, vol. I, Technical report. U.S. Dept. of the Interior,
626 Minerals Mgmt. Service, Gulf of Mexico OCS Region

627 Nowlin W. D., A. E. Jochens, S. F. DiMarco, R. O. Reid, and M. K. Howard. 2005. Low-frequency
628 circulation over the Texas-Louisiana continental shelf, p. 219–240. In W. Sturges and A. Lugo-
629 Fernandez [eds.], Circulation in the Gulf of Mexico: Observations and models. AGU Geophysical
630 Monograph Series, 161. doi:10.1029/161GM17

631 Oksanen, J., Blanchet, M. Friendly, R. Kindt, P. Legendre, D. McGlinn, P. R. Minchin, R. B. O'Hara,
632 G. L. Simpson, P. Solymos, M. Henry, H. Stevens, E. Szoecs, and H. Wagner. 2017. vegan:
633 Community Ecology Package. R package version 2.4-3. https://CRAN.R-project.org/package=vegan

634 Olson, R. J., and H. M. Sosik. 2007. A submersible imaging-in-flow instrument to analyze nano-and
635 microplankton: Imaging FlowCytobot. Limnol. Oceanogr. Methods 5: 195–203.
636 doi:10.4319/lom.2007.5.195

637 Pitcher, G., D. R. Walker, B. A. Mitchell-Innes, and C. L. Moloney. 1991. Short term variability during
638 an anchor station study in the southern Benguela upwelling system: Phytoplankton dynamics. Prog.
639 Oceanogr. 28: 39–64. doi: 10.1016/0079-6611(91)90020-M

640 R Core Team. 2016. R: A language and environment for statistical computing. R Foundation for
641 Statistical Computing, Vienna, Austria. https://www.R-project.org/

642 Rabalais, N. N., R. E. Turner, D. Justić, Q. Dortch, W. J. Wiseman, and B. K. Sen Gupta. 1996.

643 Nutrient changes in the Mississippi River and system responses on the adjacent continental shelf.
644 Estuaries 19: 386–407. doi:10.2307/1352458

645 Rabalais, N. N., R. E. Turner, and D. Scavia. 2002. Beyond science into policy: Gulf of Mexico
646 hypoxia and the Mississippi River. Bioscience 52: 129–142. doi: 10.1641/0006-
647 3568(2002)052[0129:BSIPGO]2.0.CO;2

648 Sahl, L. E., W. J. Merrell, and D. C. Biggs. 1993. The influence of advection on the spatial variability
649 of nutrient concentrations on the Texas-Louisiana continental shelf. Cont. Shelf Res. 13: 233–251.
650 doi:10.1016/0278-4343(93)90108-A

651 Schaeffer, B. A., J. C. Kurtz, and M. K. Hein. 2012. Phytoplankton community composition in
652 nearshore coastal waters of Louisiana. Mar. Pollut. Bull. 64: 1705–1712.
653 doi:10.1016/j.marpolbul.2012.03.017

654 Schiller, R. V., V. H. Kourafalou, P. Hogan, and N. D. Walker. 2011. The dynamics of the Mississippi
655 River plume: Impact of topography, wind and offshore forcing on the fate of plume waters. J. Geophys.
656 Res. Ocean. 116. doi:10.1029/2010JC006883

657 Smayda, T. J. 1970. The suspension and sinking of phytoplankton in the sea. Oceanogr. Mar. Biol.
658 Annu. Rev. 8: 353–414

659 Smayda, T. J. 1978. From phytoplankton to biomass, p. 273–279 In A. Sournia [ed.], Phytoplankton
660 Manual. Monographs on Oceanographic Methodology 6. UNESCO, Paris

661 Smayda, T. J., D. G. Borkman, G. Beaugrand, and A. Belgrano. 2004. Responses of marine
662 phytoplankton populations to fluctuations in marine climate, p. 49–58. In N. Stenseth [ed.], Marine
663 ecosystems and climate variation: The North Atlantic. A comparative perspective. OUP Oxford

664 Sosik, H. M., and R. J. Olson. 2007. Automated taxonomic classification of phytoplankton sampled
665 with imaging-in-flow cytometry. Limnol. Oceanogr. Methods 5: 204–216. doi:10.4319/lom.2007.5.204

666 Spilling, K., K. Olli, J. Lehtoranta, A. Kremp, L. Tedesco, T. Tamelander, R. Klais, H. Peltonen, and T.
667 Tamminen. 2018. Shifting diatom—dinoflagellate dominance during dpring bloom in the Baltic Sea
668 and its potential effects on biogeochemical cycling. Frontiers in Marine Science 5: 327. doi:
669 10.3389/fmars.2018.00327

670 Sylvan, J. B., Q. Dortch, D. M. Nelson, A. F. M. Brown, W. Morrison, and J. W. Ammerman. 2006.
671 Phosphorus limits phytoplankton growth on the Louisiana shelf during the period of hypoxia
672 formation. Environ. Sci. Technol. 40 (24): 7548–7553. doi: 10.1021/es061417t

673 Tilstone, G. H., B. M. Miguez, F. G. Figueiras, and E. G. Fermin. 2000. Diatom dynamics in a coastal
674 ecosystem affected by upwelling: Coupling between species succession, circulation and
675 biogeochemical processes. Mar. Ecol. Prog. Ser. 205: 23–41. doi:10.3354/meps205023

676 Walker, N. D. 2001. Wind and eddy-related circulation on the Louisiana/Texas shelf and slope
677 determined from satellite in situ measurements: October 1993-August 1994. U.S. Dept. of the Interior,
678 Minerals Mgmt. Service, Gulf of Mexico OCS Region

679 Walker, N. D., S. Myint, A. Babin and A. Haag. 2003. Advances in satellite radiometry for the
680 surveillance of surface temperatures, ocean eddies and upwelling processes in the Gulf of Mexico using
681 GOES-8 measurements during summer. Geophys Res Lett, 30: 1854. doi:10.1029/2003GL017555

682 Walker, N. D., W. J. Wiseman, L. J. Rouse, and A. Babin. 2005. Effects of river discharge, wind stress,
683 and slope eddies on circulation and the satellite-observed structure of the Mississippi River plume. J.
684 Coast. Res. 216: 1228–1244. doi:10.2112/04-0347.1

685 WHPO. 1994. WHPO Operations and Methods. WOCE Hydrographic Office Report 91/1, as revised.

686 WOCE Hydrographic Program Office, Woods Hole, MA

687 Williams, A. K., A. S. McInnes, J. R. Rooker, and A. Quigg. 2015. Changes in microbial plankton
688 assemblages induced by mesoscale oceanographic features in the Northern Gulf of Mexico. PLoS One
689 10 (9): e0138230. doi:10.1371/journal.pone.0138230

690 Wiseman, W. J., N. N. Rabalais, R. E. Turner, S. P. Dinnel, and A. Macnaughton. 1997. Seasonal and
691 interannual variability within the Louisiana coastal current: Stratification and hypoxia. J. Mar. Syst. 12:
692 237–248. doi:10.1016/S0924-7963(96)00100-5

693 Zavala-Hidalgo, J., S. L. Morey, and J. J. O'Brien. 2003. Seasonal circulation on the western shelf of
694 the Gulf of Mexico using a high-resolution numerical model. J. Geophys. Res. 108: 3389.
695 doi:10.1029/2003JC001879

696 Zavala-Hidalgo, J., A. Gallegos-García, B. Martínez-López, S. L. Morey, and J. J. O'Brien. 2006.
697 Seasonal upwelling on the Western and Southern Shelves of the Gulf of Mexico. Ocean Dyn. 56: 333–
698 338. doi: 10.1007/s10236-006-0072-3